



## Electronic Structure, Magnetic and Optical properties of Fe<sub>2</sub>MnZ (Z=Si, Ge, Sn, Ga)

InamulHaqWani<sup>1</sup>, Vikas Sharma<sup>2</sup>, Akshaysambyal<sup>3</sup>, MonitaBhat<sup>4</sup>, Rajesh Gupta<sup>5</sup>, Sushila<sup>6</sup>

Department of Physics, Vivekananda Global University Jaipur, Rajasthan, India<sup>1,6</sup>

Department of Physics Maulana Azad Memorial College, Jammu, Jammu and Kashmir, India<sup>2,3,4,5</sup>

Corresponding Author: [Inamwani123@gmail.com](mailto:Inamwani123@gmail.com)

Keywords: Full Heusler Alloy, Electronic Structure, Magnetic Properties, Optical Properties

### Abstract:-

The article describes the electronic structure, magnetic and optical properties of bulk Fe<sub>2</sub>MnZ (Z= Si, Ge, Sn, Ga) of full heusler alloy. The value of total magnetic moment is  $3\mu_B$  for Fe<sub>2</sub>MnSn and Fe<sub>2</sub>MnGe at their equilibrium lattice constant and follows Slater-Pauling curve. Fe<sub>2</sub>MnSn posses the largest magnetic moment among the three with the value of  $5.73\mu_B$  at equilibrium lattice constant. The magnetic and optical properties of Fe<sub>2</sub>MnGa of heusler alloy are discussed in terms of energy band calculation for ordered FCC and L<sub>21</sub> type structure.

DOI Number: 10.14704/nq.2022.20.11.NQ66252

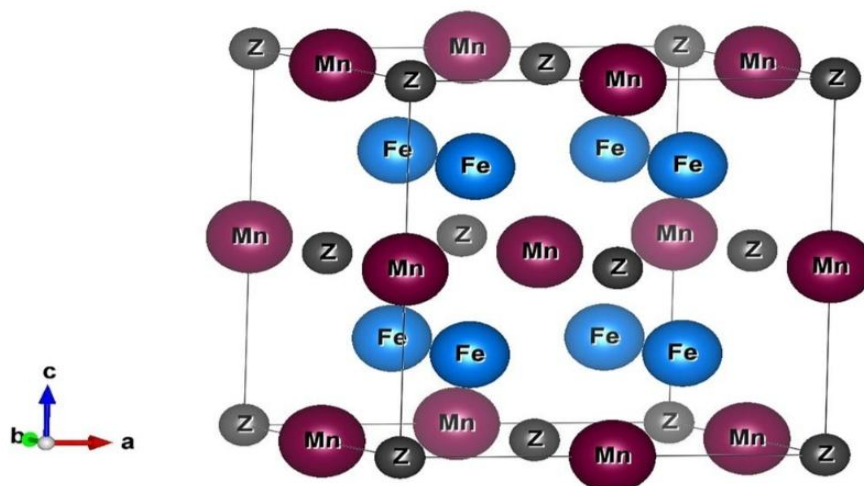
NeuroQuantology 2022; 20(11): 2527-2535

### Introduction:-

Heusler alloys possessing half metallic ferromagnetic nature. It has high spin polarization due to presence of a gap Fe<sub>2</sub>YZ Heusler alloy with Y which is transition metal (Mn) and with Z as a semiconductor. Good thermoelectric and magnetic properties can be calculated by theatrical calculation of the

electronic structure in magnetic order Fe<sub>2</sub>MnZ heusler alloy. Yang founded that magnetic moment is affected with pressure in Fe<sub>2</sub>MnAl. The structural transformation in Fe<sub>2</sub>MnGa is bcc and the electronic structure of Fe<sub>2</sub>MnGa alloy is with Fcc-type. Now, the electronic structural, magnetic and optical properties of Fe<sub>2</sub>MnZ (Z= Si, Ge, Sn and

2527



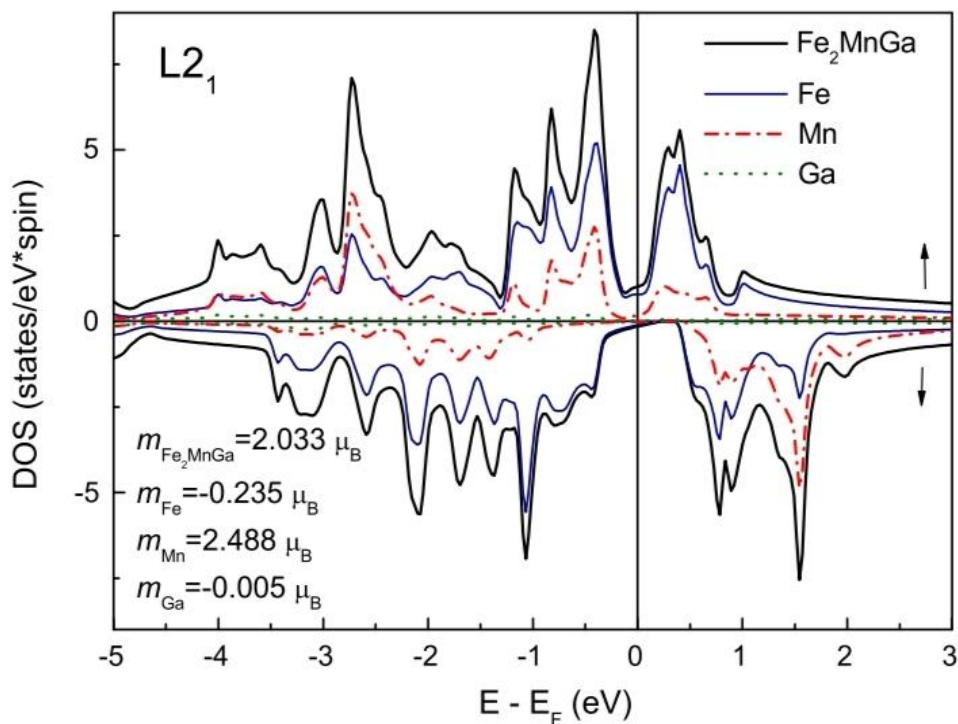
Ga).

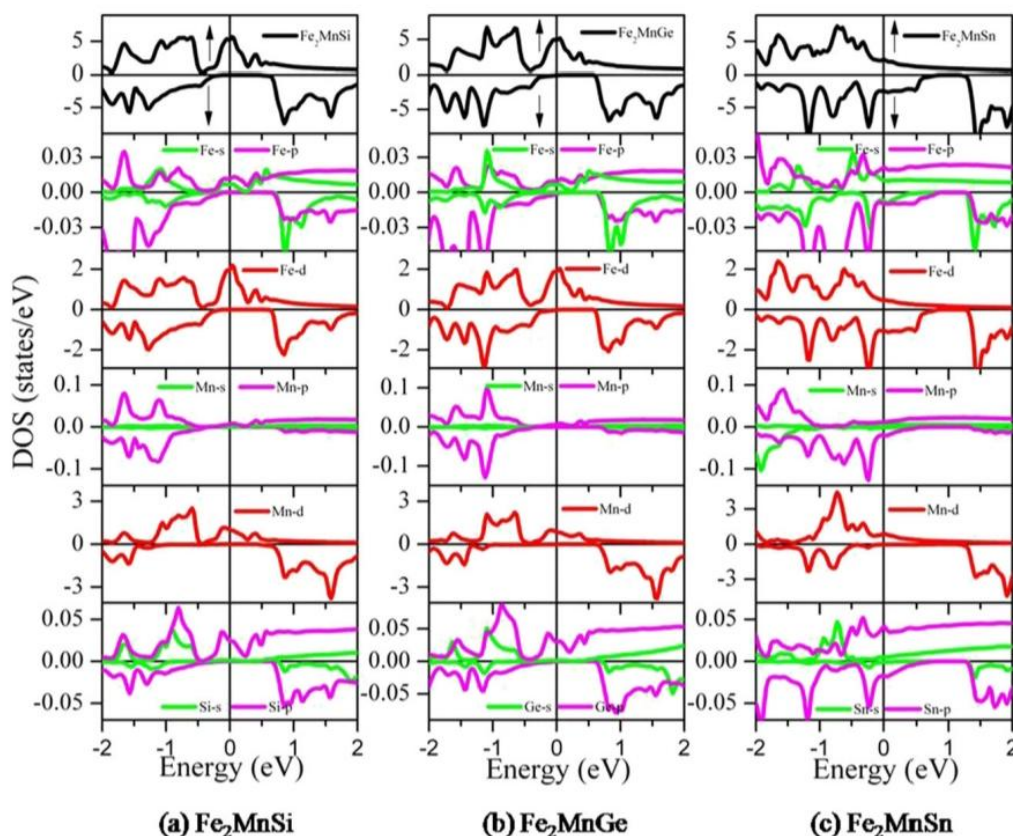
### Electronic Structural Properties :-



It can be seen that the main contribution is due to the Fe and Mn atoms, which have strongly hybridized states: the most intense DOS peaks formed by both Fe and Mn states coincide in terms of energy. Furthermore, we observe that a main contribution to those hybridized states is due to the Fe and Mn 3d states indicating the covalent character of their interaction. DOS of sp elements of Si, Ge, and Sn have contributed to the lower valence state and higher conduction state in both majority and minority spin bands. The Ga contribution to the total DOS is small i.e. Ga atoms form basically ionic bonds with surrounding atoms. Alloys are said to be true half metallic when value of SP is 100% and is achieved when any one of the DOS from majority and minority spins is equal to zero and other is not equal to zero at  $E_F$ . Now Fe<sub>2</sub>MnSi shows half-metallic behavior where Fe<sub>2</sub>MnGe and Fe<sub>2</sub>MnSn are not

fully half metallic. The calculated density of electronic states (DOS) for Fe<sub>2</sub>MnGa alloy in L2<sub>1</sub>-phase shows that spin up and spin down states are strongly polarized, since separate peaks of the up and down states. The calculated DOS of spin-up states at  $E_F$  is 1.009, while spin-down  $E_F$  is 0.152. The minority spin band in Fe<sub>2</sub>MnSi shows band gap of 0.5eV at  $E_F$ . The minority spin band in Fe<sub>2</sub>MnGe shows band gap of 0.45 eV at  $E_F$ . The minority spin band in Fe<sub>2</sub>MnSn shows band gap of 0.35eV at  $E_F$ . As this shows decreasing order at Fe<sub>2</sub>MnSi>Fe<sub>2</sub>MnGe>Fe<sub>2</sub>MnSn. The calculated densities of electronic states for Fe<sub>2</sub>MnGA alloy is ferro- and ferromagnetic order. The DOS of Fe<sub>2</sub>MnGe and Fe<sub>2</sub>MnSN shows metallic and ferromagnetic behavior at majority spins.





**Optical Properties:-**

In general, Optical properties of semiconductor materials are observed to exhibit a metal-like behavior at very low frequencies and insulator like at very high frequencies necessitating the study of optical properties with variation in the incident photon energy as has been done in the present work. The results are shown in fig. The main features of the optical absorption spectra are the high level of interband absorption peaks of interband absorption which are observed at different energy points for three alloys (Fe<sub>2</sub>MnZ, Z= Si, Ge, and Sn) in the whole spectral range (0-13ev) studied, namely, infrared (IR) (1.24MeV to 1.7ev), visible (1.7 to 3.3ev), and UV (3.3 to 1.24ev). Overall, peaks of different optical Parameter are seen at a lower Photon energy range of energy for Fe<sub>2</sub>MnSi. The existence of low-energy gaps in the band spectra of alloys (Fe<sub>2</sub>MnZ, Z= Si, Ge, Sn) are correlated to the

presence of peaks of these alloys are also found in the energy ranges corresponding to visible and UV parts of spectrum.

Optical conductivity spectra, fig shows that two major peaks are observed for the alloys Fe<sub>2</sub>MnZn (Z= Si, Ge, Sn) in the energy range of 2-3 and 7-10ev. The value of Fe<sub>2</sub>MnSn is the least among Fe<sub>2</sub>MnZ and shifts towards lower energy side while Fe<sub>2</sub>MnSi shows high energy points. This shows that of three alloys. Fe<sub>2</sub>MnSn is least conductive in visible region.

The trend of reflectivity R (σ) as function of photon energy in fig indicates that all three samples how major peaks below 3ev in IR and visible light region and above 8ev in the UV region. The value of reflectivity is more than 50% for alloys in a range of energy between 0ev and 4ev and from 8ev onwards in the UV region.



Trends of energy loss  $L(\omega)$  and absorption coefficient  $I(\omega)$  with the incident photon energy show that absorption coefficient and energy loss increase as incident photon energy increases. Maximum energy loss occurs have above 10eV in the UV region for the alloys with Fe<sub>2</sub>MnSn shows highest energy loss. This implies that reflectivity is minimum at the point at which energy loss is maximum and vice-versa.

The complex dielectric function  $E(\omega)$  is  $E(\omega) = E_1(\omega) + iE_2(\omega)$

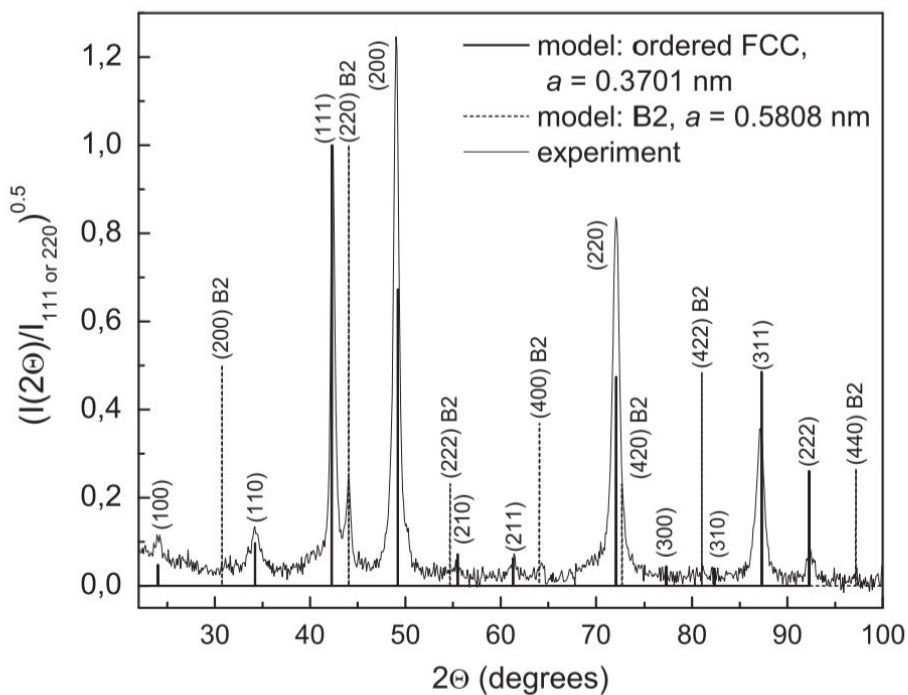
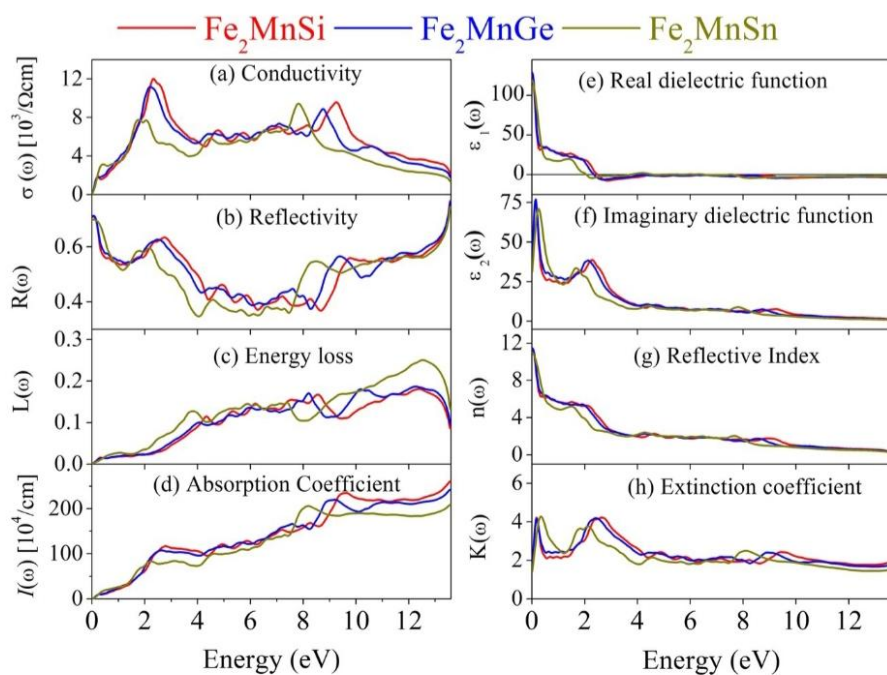
Here  $E_1(\omega)$  and  $E_2(\omega)$  are real and imaginary parts of dielectric function related to the polarization and energy loss resp. and the characteristics freq. is called plasma freq. and defined as that freq. at which the real part of the dielectric function vanishes on  $E_1(\omega) = 0$ . The values  $\omega_p$  of are in the order Fe<sub>2</sub>MnSn > Fe<sub>2</sub>MnGe > Fe<sub>2</sub>MnSi. The peaks of the real and imaginary parts are found in the IR and visible region for alloys. Behavior of  $E_2(\omega)$  for Fe<sub>2</sub>MnSi, Fe<sub>2</sub>MnGe, Fe<sub>2</sub>MnSn alloys is identical with that of  $R(\sigma)$  with respect to incident photon energy. Negative values of  $E_1(\omega)$  shows a metallic behavior of all three alloys in visible and UV regions. These alloys have potential for use in optical filters or shielding devices at different freq. region. The value of  $E_1(\omega)$  shows energy absorption is high in the IR region.

Refractive index  $n(\omega)$  as a function of photon energy of all three alloys. Value of  $n(\omega)$  at zero frequency is 11.33, 11.47 and 11.00 for Fe<sub>2</sub>MnSi, Fe<sub>2</sub>MnGe and Fe<sub>2</sub>MnSn resp. and

decreases with increase in photon energy. Fe<sub>2</sub>MnSn shows lowest value of  $n(\omega)$  among the three at lower energy points from visible to UV region. In the IR region peaks of  $K(\omega)$  for Fe<sub>2</sub>MnSi and Fe<sub>2</sub>MnGe overlap while those of Fe<sub>2</sub>MnSn are at high energy. In visible and UV regions peaks of  $K(\omega)$  for Fe<sub>2</sub>MnSi and Fe<sub>2</sub>MnGe. The maximum value of  $K(\omega)$  is 4 for alloys and decreases with increase in photon energy toward UV region.

In XRD analysis shows in Fe<sub>2</sub>MnGa addition to the fundamental [111, 200, 220, 311 and 222] diffraction lines a set of super structure diffraction peaks [100, 110, 210, and 211] clearly indicates the formation of ordered structure in the alloy Fe<sub>2</sub>MnGa. At the sometime, as well as these diffraction lines, additional reflections at  $2\theta = 44.05$  and  $99.27$ . Signify the presence of second phase. These can be assigned to the fundamental (220) and (440) reflection of A2-(Or B2 or L21 phase with lattice constant  $a = 0.5808$ nm), with the volume fraction below 10%. The experimental lattice parameters of Fe<sub>2</sub>MnGa HA for Fcc- ( $a = 0.3701$ nm) and A2( B2 or L21)- phase ( $a = 0.5808$ ) are similar to the calculated parameters  $a = 0.3644$  or  $0.666$ nm for fcc-phase or  $a = 0.57$ nm for L21-Phase, are in good agreement with the data  $a = 0.5685$ nm or  $a = 0.5688$ nm. It should be mentioned here that the XRD spectrum as milled powder of Fe<sub>2</sub>MnGa did not show any A2-phase related peaks.





**Magnetic properties:-**

The calculated value of total and individual magnetic moment for  $Fe_2MnZ$  is shown in table. Magnetic moment of Fe increases in the presence of Sn and is the same for Mn atom in all three alloys. While the magnetic moment of the Z-atom is negative and negligible. According to Slater-Pauling curve. The magnetic moment per unit cell in multiples of Bohr magneton ( $\mu_B$ ) is given by  $M_{total} = n - 24$ .

Total and partial magnetic moment in terms of  $\mu_B$  of  $Fe_2MnZ$  Heusler alloys

Sample	Total	2*Fe	Mn
Z			
$Fe_2MnSi$	3.00	0.53	2.49
-0.01			
$Fe_2MnGe$	3.00	0.38	2.61
-0.01			
$Fe_2MnSn$	5.73	3.47	2.45
-0.07			

Where N denotes valence electrons in the unit cell. For  $Fe_2MnZ$ , there are a total of 27 valence electrons in the unit cell of  $Fe_2MnZ$ . For this reason the magnetic moments are the expected from SPC is  $3\mu_B$  for all three alloys. While the calculated magnetic moments are the same as that predicted by SPC  $Fe_2MnSn$  is 5.73. A calculation of the dependence of the magnetic moment on the value of the lattice constant makes the trend clear. To further explore this aspect we have calculated variation in total and partial magnetic moments with respect to  $a_0$ .

For range of  $a_0$  from 5.30 to 5.85 Å the total magnetic of all three alloys is  $3\mu_B$  and remain constant, which follows the Slater-Pauling rule for full Heusler alloys. However variation in the individual magnetic moments of Fe and Mn are brought about due to the change in the separation on a change in the lattice constant which affects the interaction and thus hybridization 3d electron is present. Magnetic moment of Fe decreases while it increases for

Mn with increase in lattice constant for all alloys. Magnetic moment of Z atoms remains almost zero and doesn't effectively contribute to the total Magnetic moment of  $Fe_2MnSi$  becomes higher than  $3\mu_B$  and does not follow the Slater Pauling rule and Fe moment starts to increase. Although we have plotted the magnetic moment for lattice constants higher than 5.85Å for  $Fe_2MnSn$  alone almost the same behavior is observed for  $Fe_2MnSi$  and  $Fe_2MnGe$ . However the equilibrium lattice constant for  $Fe_2MnSn$  is 6.01Å and is the reason that the calculated magnetic moment is much larger than that predicted by SPC. The sudden increase in the lattice parameter after 5.85Å is mainly due to the sharp increase in the moment of the Fe atom due to change in hybridization of the 3d electron brought about by the change in lattice parameter the majority and minority DOS with variation in lattice constant  $a_0$  for  $Fe_2Mn(Si, Ge, Sn)$ . The majority spin DOS at Fermi energy levels is almost the same for or 4.86 $\mu_B$  at T=2k and H=10<sup>7</sup>. Some what smaller than predicted by the calculation i.e 6.10 $\mu_B$ , but nearly two times larger than that phase melt-spin stoichiometric  $Fe_2MnGA$  ribbon  $M_s=58 \text{ emu g}^{-1}$  (at T=5K and H=5T). The origin of this discrepancy may be related partly to the degree of atomic disorder in our bulk sample and ribbons, as well as to the presence of some A2-(B2- or L2<sub>1</sub>) phase with smaller magnetic moment [13,24,25]. At the same time insignificant deviation from stoichiometry weakly affects the saturation magnetization of  $Fe_2MnGa$  alloys near 2:1:1 stoichiometry  $M_s=93.8 \text{ emu g}^{-1}$  (at T=5k and H=13T).

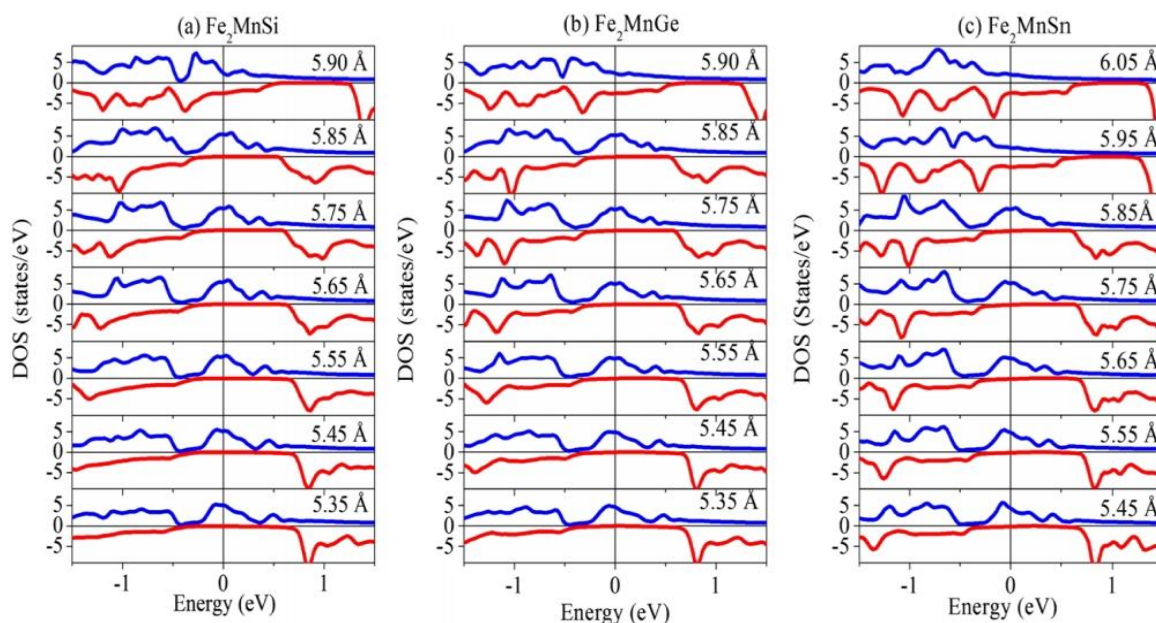
On the other hand for these slightly off stoichiometric  $FeMnGa$  alloys, the magnetization hysteresis loop for 100≤T≤170K temperature ranges. Clearly show the presence of martensitic transformation from parent PM to martensitic FM phase. However, unlike the afford



mentioned case, M(H) dependencies For Fe<sub>2</sub>MnGa bulk alloy do not show any traces of hysteresis in the 2-400K temperature range, indicating the absence of martensitic transformation.

The first peculiarity can be attributed to the FM-PM transition with Curie temperature  $T_C=800K$  all range of Lattice constants for all three alloys

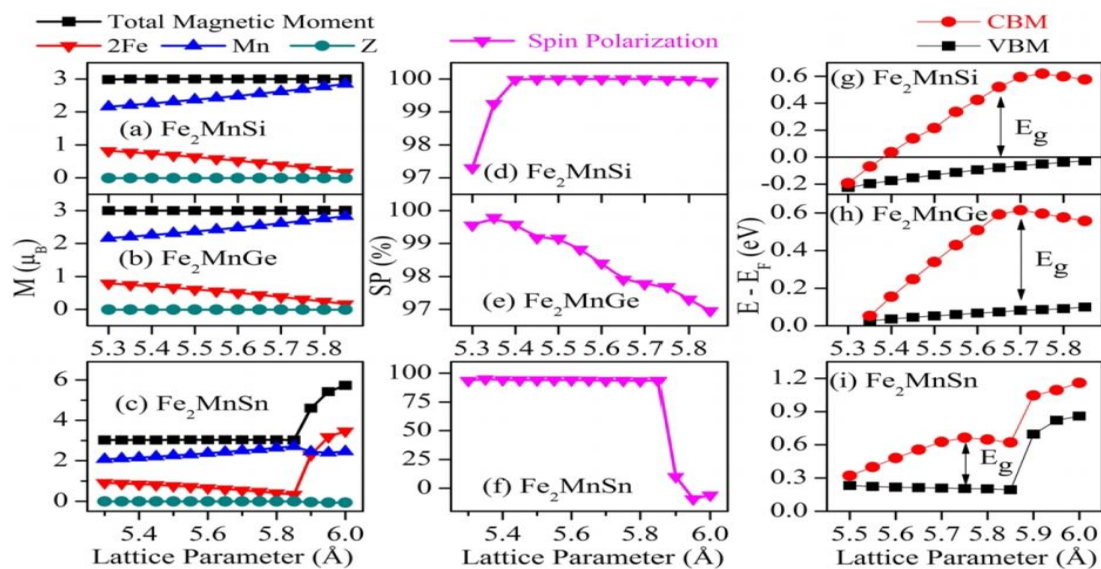
while it shift towards the valence state in minority spin DOS on decrease in the lattice constant. This indicates that all three alloys exhibit a semiconductor behavior at ranges of lattice constant lesser than the equilibrium lattice constant in the minority DOS.



The temperature dependence of magnetization of bulk Fe<sub>2</sub>MnGA alloy taken at different magnetic field behave in a noticeably different way. At low magnetic field, the zero field cooled (ZFC) branch of the M(T) curve for Fe<sub>2</sub>MnGa alloy rapidly inc. with temperature, intersecting the zero-line at T=60K. However at  $1 \text{ emu}^{-1}$  the field cooled (FC) M (T) curve combines two different regions with a decrease and increase in magnetization upon warming. At  $1 \text{ emu}^{-1}$  magnetization insignificantly increases with temperature. At rather high magnetic field  $1 \text{ emu}^{-1}$  the magnetization M(H) of Fe<sub>2</sub>MnGa alloy behaves typically for ferromagnetic an inc.

in temp. Curve a dec. in magnetization. The rapid inc. in magnetization at  $t=250K$  from nearly zero up to  $29.2 \text{ emu}^{-1}$  on ribbon warning at  $1 \text{ emu}^{-1}$  was attribute by the author to the meta-magnetic transformation in the alloy from AFM to FM phase. No structural transformation at this temperature was observed. The AFM to FM transition in the ribbon is evidenced by the change in the field dependence of magnetization M(H) i.e. an appearance of the linear part of the M(H) curve within the AFM region and its asymmetry with respect the origin.





The FC temperature dependence of magnetization of our bulk Fe<sub>2</sub>MnGa alloy obtained for emug<sup>-1</sup> consist of two clear parts i.e. decrease and increase in magnetization with increase in temperature. Such behavior can be explained by different magnitudes and M(T) dependencies of Fcc and Bcc type ordered phases in the alloy. Indeed according to the results of our calculation the magnetic moment of the FM FCC-phase is more than three times large than that of the L<sub>21</sub> phase, At higher there as the M(T) dependence of the BCC ordered impurity phase is masked by the M(T) of the dominant parent phase. The experimental value of the saturation magnetization of our bulk Fe<sub>2</sub>MnGa alloy.

**Conclusion:**

- 1- This study shows that the total magnetic moment of Fe<sub>2</sub>MnZ (Z=Si, Ge, Sn, Ga) remains 3μ<sub>B</sub>.
- 2- Good optical conductivity and reflectivity in various regions of the electromagnetic spectrum are observed in these alloys.

- 3- They show dielectric to metallic transition which has a potential for use in optical filters and photo electronics devices.
- 4- FeMnGa with a curie temperature of T<sub>c</sub>=800K and a saturation magnetization of 4,86μ<sub>B</sub> F,U-1 crystallizes in the FCC ordered lattice of L<sub>12</sub>.

**References:**

- 1- Yin, M., Nash, P., Chen, S.: Enthalpies of formation of selected Fe<sub>2</sub>YZ heusler compounds. Intermetallics 57, 34-40 (2015)
- 2- Graf T, Felser C, Parkin SSP. Prog Solid State Chem 2011;39(1)
- 3- Kokorin VV, Martynov VV, Chernenko Va. Scr Metal Mater 1992;26:295
- 4- Galanakis I, Dederichs PH, Papanikolaou N. Phys Rev B 2002;66:174429





- 5- Kikalj A. Comput Mater Sci 2003;28:155
- 6- Thee JY. J Korean PhysSoc 2003;43:792
- 7- Blaha P, Schwarz K, Madsen GKH, Kvasnicka D, Luitz J. WIEN2k, an augmented plane wave + local orbitals program for calculating crystal properties. Karl-heinz Schwarz, Techn. UniversitAat Wien, Wien; 2001.
- 8- M. Pugaczowa-Michalska, A. Go, L. Dobrzynski, Phys. Status Solidi B 242 (2) (2005) 463.
- 14-
- 9- S.M. Azar, B.A. Hamad, J.M. Khalifeh, J. Magn. Magn. Mater. 324 (2012) 1776–1785
- 10- A.H. Reshak, Z. Charifi, H. Baaziz, , J. Magn. Magn. Mater. 326 (2013) 210–216.
- 11- D. Nanto, D.-S. Yang, S.-C. Yu, Physica B 435 (2014) 54–57
- 12- K.M. Wong, S.M. Alay-e-Abbas, Y. Fang, A. Shaukat, Y. Lei, J. Appl. Phys. 114 (2013) 034901.
- 13- W. Kohn, L.J. Sham, Phys. Rev. A 140 (1965) 1133

